Avraam A. Konstantinidis, Konstantinos Michos and Elias C. Aifantis*

On the correct interpretation of compression experiments of micropillars produced by a focused ion beam

DOI 10.1515/jmbm-2016-0009

Abstract: The modest goal of this short note is to shed some light on the correct interpretation of micro/nanopillar compression experiments. We propose a modification of the way the stress-strain response in such experiments is calculated, aiming at answering open questions pertaining to discrepancies between the elastic moduli values calculated through micropillar compression experiments with those of the bulk materials, as well as the brittle-to-ductile transition in bulk metallic glasses (BMGs) when the size of the pillars is reduced below a certain threshold value.

Keywords: pillar compression; size effects; stress-strain response.

1 Introduction

Miniaturization of machines and components has rendered understanding the mechanical behavior of small material volumes crucial for their design and operation. Quantifying the stress-strain behavior of small material volumes that is usually intermittent and jerky is quite a challenge. Initially, indentation techniques were used for determining the mechanical properties of small volumes [1]. But the rather complex stress and strain fields involved in the indentation tests made even more necessary the development of a novel test for determining material behavior at small volumes. This test is the micro/nanopillar compression test. During this test, a nanoindenter with a flat punch tip is used for compressing cylindrical pillars with diameters in the nano or micro regime that are produced with the focused ion beam (FIB) technique in single crystal [2–9], nanocrystalline [10], and nanoporous [11, 12] metals.

Although the micropillar compression test was developed as a counterpart of nanoindentation for measuring elastic constants such as the modulus of elasticity, there are a number of experimental works in the literature that report stress-strain curves of micropillar compression tests of various materials showing a discrepancy between the initial slope of the compressive stress-strain graphs and the Young's modulus value of their bulk counterparts. These discrepancies have been attributed to the taper of the pillars due to the FIB process, misalignment between the pillar and the indenter flat punch, sink-in phenomena, etc [13].

The modest aim of this short note is to provide an alternative interpretation of the micropillar compression measurements. It will be shown that it is not the way the compression measurements were conducted, but rather the way the reported stress-strain graphs were calculated that caused the aforementioned discrepancies between the measured slopes in the initial elastic region and the values of the elastic moduli of the respective bulk materials.

2 Formulation of the proposed pillar compression interpretation

2.1 Motivation

In order to model for the first time, qualitatively as well as quantitatively, the intermittent plastic behavior during nickel (Ni) micropillar compression experiments [6], a stochasticity-enhanced gradient plasticity model was implemented with a cellular automaton [13], with the simulation results being in very close agreement to the experimental ones. In this work [13], in order for the simulation results to model the experimental ones, instead of the Young's modulus of Ni (~200 GPa) for the elastic part of the stress-strain graphs, a much lower value was used,

***Corresponding author: Elias C. Aifantis,** Aristotle University, Thessaloniki 54124, Greece; Michigan Tech. University, Houghton MI 49931, USA; ITMO University, St. Petersburg 197101, Russia; and BUCEA, Beijing 100044, China, e-mail: mom@mom.gen.auth.gr
Avraam A. Konstantinidis and Konstantinos Michos: Aristotle University, Thessaloniki 54124, Greece

corresponding to the initial slope depicted in the reported experimental stress-strain graphs. It should also be noted here that the slopes of the elastic part of all the experimental measurements in [6] should be the same, irrespective of the pillar's size. The authors of [6] do not present an explanation for this difference of the slopes of the elastic regions with the actual modulus of elasticity of Ni other than misalignment between the pillar and the indenter flat punch.

The aforementioned discrepancy provided motivation to propose a new interpretation of the compression measurements. It is thought that in the aforementioned works [2–12], the differences between the measured and the actual modulus values are not caused by errors in the respective measurements, but the main cause is the way that the reported stress-strain curves are calculated from the load-displacement measurements during micropillar compression. This new interpretation of pillar compression measurements is described in the next section.

It should be also noted, however, that this discrepancy between elastic moduli and the slopes of the elastic part in the stress-strain curves has concerned researchers before. Greer et al. [14] employed the Sneddon correction to account for sink-in effects, assuming that the pillar is pushing as a nanoindenter into the substrate, by also satisfying the criterion of having an initial slope equal to the elastic modulus. The pillar and substrate were treated like two distinct materials and a comparison between measured stiffness of FIB-produced pillars and the theoretically predicted values showed satisfactory agreement.

Fei et al. [15] state that issues of tapering, misalignment, and sink-in phenomena affect measurements, and to this cause, produce a finite element method to assess the accuracy of the microcompression measuring technique, taking into account the Sneddon correction. The total displacement was measured by microcompression experiments as the combined effect of the indenter, pillar, and substrate strain. It was concluded that the Sneddon correction can tackle sink-in phenomena, even for thick substrates, regardless of the substrate material, as the finite element method (FEM) produces negligible substrate strains. Still, the microcompression method is not deemed suitable for measuring the elastic modulus. This is attributed to the stress state not being uniform because of tapering angles. Another issue mentioned was that the Sneddon correction requires a half-space, which is not always valid for microcompression tests.

2.2 Theoretical stress-strain calculation

In every micropillar compression experiment, the measured quantities are the load P, with which the flat punch indenter pushes the upper surface of the pillar, and the deformation h of the pillar, while the stress and strain quantities are calculated from P and h, respectively. In Figure 1, a pillar compression configuration is depicted. A small material volume of thickness H is used for producing micropillars of varying sizes through the FIB technique. The region marked as A_c is the specimen part that is cut-off by the FIB in order for pillars with different diameters and heights, e.g. the ones marked with A_1 and A_2 in Figure 1, to be left protruding from the volume marked as A_s, which is acting as a "substrate" to the pillars.

In all the aforementioned works [2–12], the stress is calculated by dividing the load P exerted on the pillar's upper surface by this surface, while the strain is calculated by dividing h with the respective pillar height, e.g. H_p. It should be noted that this calculation provides the local strain and stress values at each point of the "pillar" protruding from the specimen's surface.

As can be seen from Figure 1, the material volume being compressed by the indenter flat punch is not the pillar of height H_p, but a pillar of height H_p+H_s, marked with dashed lines. It can also be seen that the load P is exerted at the upper surface of the material on an area equal to the pillar's surface, but at the bottom of the material on an area equal to the surface area of the whole sample. This means that there is a distribution of local stresses along the sample height, as there are two very different areas of load application, i.e. the area πD_p^2 at the top, with D_p denoting the diameter of the pillar at hand, and at the bottom of the sample the area A of the "substrate". In addition, there is a distribution of local strains

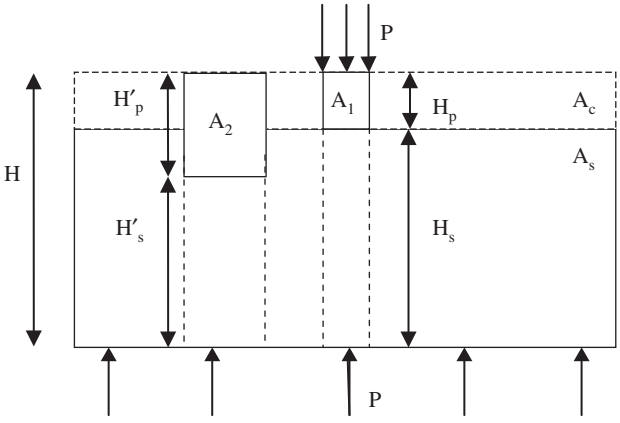

Figure 1: Schematic of a micropillar compression test.

along the compressed specimen height. This comes from the fact that the elastic moduli of the "pillar" and the "substrate" are the same; thus, at least during elastic loading, one should expect that

$$\frac{\sigma_p}{\varepsilon_p}=\frac{\sigma_s}{\varepsilon_s}\Rightarrow\varepsilon_s=\varepsilon_p\frac{\sigma_s}{\sigma_p}, \quad (1)$$

with ε_p denoting the local strain at each point of the "pillar" (the strain calculated and reported in the aforementioned works) [2–12] and ε_s denoting the local strain at each point of the "substrate", while σ_p and σ_s are the local stress values at the "pillar" and "substrate", respectively, calculated as

$$\sigma_p=\frac{P}{\pi D_p^2},\ \sigma_s=\frac{P}{A}=\frac{\sigma_p\pi D_p^2}{A}. \quad (2)$$

In the next section, two examples of applying the proposed formulation when calculating the stress-strain response of micropillars under compression are given.

3 Examples of "corrected" mechanical response

In this section, some examples of the correct interpretation of pillar compression measurements as described in Section 2.2 are given. It is noted that although the proposed "correction" can be applied in all reported stress-strain curves which show a difference between the slope of the initial elastic part and the value of the modulus of elasticity, the thickness of the material undergoing FIB treatment for the construction of the pillars is needed herein. Thus, the examples below concern experimental works where apart from the stress-strain curves, an indication of the thickness H of the material acting as a "substrate" to the pillars is reported.

3.1 Compression of Ni micropillars

A number of pure Ni micropillars were subjected to micro-compression tests using a flat diamond indenter tip in [6]. All of them were derived from a single crystal Ni specimen using FIB and featured diameters between 1 and 40 μm and aspect ratios between 2:1 and 3:1. Figure 2 shows the resulting engineering stress-strain graphs from [6].

The initial slope of the curves (defined by a straight line) has a value of 50 GPa, which is significantly lower

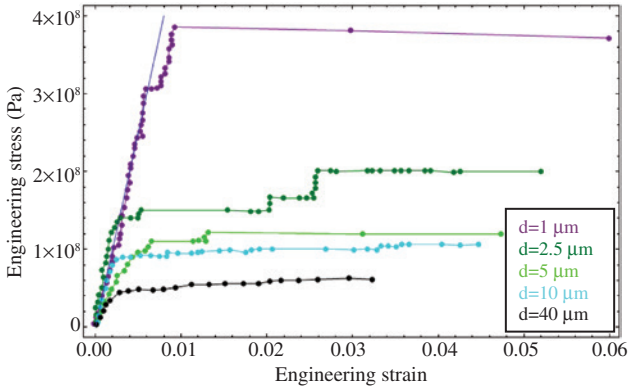

Figure 2: Engineering stress-strain graphs of pure Ni micropillar compression [6]. The slope of the straight line provides a modulus value of 50 GPa.

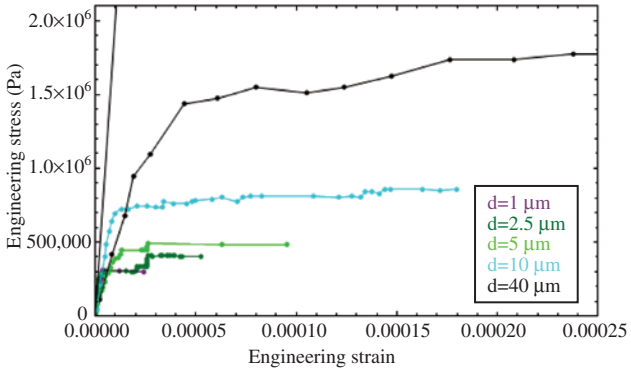

Figure 3: Recalculated engineering stress-strain graphs of pure Ni micropillar compression using Eq. 3. The slope of the straight line provides a modulus value of 200 GPa.

than the elastic modulus of bulk Ni (~78 GPa [6]). It is also evident that specimens of different diameters exhibit different initial slopes. While the authors include a detailed analysis on the form of the elicited curves, there is no comment on the slope of the graph at the elastic part. However, misalignment issues can be excluded due to the inclusion of a goniometer sample stage.

To this cause, these curves are recalculated using Eq. (3), thus, taking into account not only the contact area between the indenter tip and micropillar but also the area on the bottom of the substrate where load is also applied (3×3 mm [6]). The height of the pillar is also taken into account (7.4 mm substrate height plus specimen height [6]). The corrected graph is presented in Figure 3. It is noted that the same color code was used for the differently sized specimens as in the original paper [6].

The recalculated graph exhibits stress-strain responses with initial slopes of about 200 GPa, a value

very close to the elastic modulus of bulk Ni. Also, the slopes no longer exhibit divergence initially.

It should be noted that the corrected graph presents the curves in reverse order, i.e. pillars of greater size exhibit higher yield stresses, a fact that, at first glance, contradicts the "smaller is stronger" concept. But this is not the case actually. In order to understand this, one should take into account that the FIB method produces pillars by removing the substrate material around a designated area, instead of depositing on it. As a result, in order to produce larger pillars, the "effective" volume of the "substrate" material, i.e. H_sA_s in Figure 1, is getting smaller. Thus, it is actually the specimen with the larger pillars that include a smaller "effective" volume, and not vice versa, as it can be mistakenly thought at first glance.

3.2 Compression of metallic glasses micropillars

Stress-strain curves have been reported for size-dependent microcompression tests on palladium-silicon (PdSi) metallic glass columns [16]. More specifically, a 5.5 μm-thick $Pd_{77}Si_{23}$ metallic glass thin film was fabricated by Argon ion-beam sputtering onto a Si-(100) substrate. Micro and nanocolumns were cut with FIB, with diameters ranging between 200 nm and 2000 nm at a fixed aspect ratio of height/diameter ~3 [16].

In their experimental measurements, shown in Figure 4, the authors attribute the low slope of the initial part of the stress-strain curves for very small samples to the inevitable top-rounding originating from the FIB-milling procedure [17], having, as a result, small samples (<300 nm) deform plastically at lower engineering stress. The authors also note an unexpected change of elastic slope as a function of sample size, not due to size-dependent elasticity, as well as an intermittent-to-smooth flow behavior.

We apply below the proposed formulation to the experiments of [16]. Using Eq. (3) with H=5.5 μm and various values for H_p, the stress-strain graph of Figure 4 is now transformed to the one shown in Figure 5.

Comparing the graphs shown in Figures 4 and 5, it can clearly be seen that in contrast to the reported results [16], the recalculated results show that all pillars, irrespective of diameter, have the same initial slope, calculated as 90 GPa, which is very close to the modulus of elasticity of the metallic glass measured as 86 GPa using nanoindentation [16].

Another study conducted by Dubach et al. [18] included microcompression of 0.3, 1, and 3 μm diameter samples made of a zirconium (Zr)-based metallic glass ($Zr_{41.2}Ti_{13.8}Cu_{12.5}$-$Ni_{10}Be_{22.5}$). The total specimen height that was taken into account for the correction was 3 mm and the aspect ratios (height/diameter) varied from 2 to 2.5. Slight tapering of 2°–4° is mentioned. The obtained results are presented in Figure 6.

Taking into account the height of the substrate and Eq. 3, the recalculated graph is presented in Figure 7. It is evident that now the initial slopes are very similar and feature values of 90 GPa. The bulk elastic modulus of the above-mentioned metallic glass is considered to be 96 GPa by the authors of [18], as mentioned in [19].

4 Conclusions

This work aims at presenting the issues involved with the calculation of stresses and strains in compression experiments of FIB-manufactured micropillars. The corrections proposed are based on the consideration that

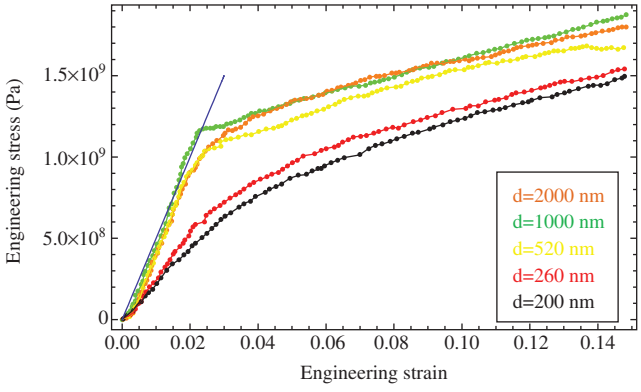

Figure 4: Engineering stress-strain graphs during $Pd_{77}Si_{23}$ metallic glass micropillar compression [16]. The slope of the straight line provides a modulus value of 50 GPa.

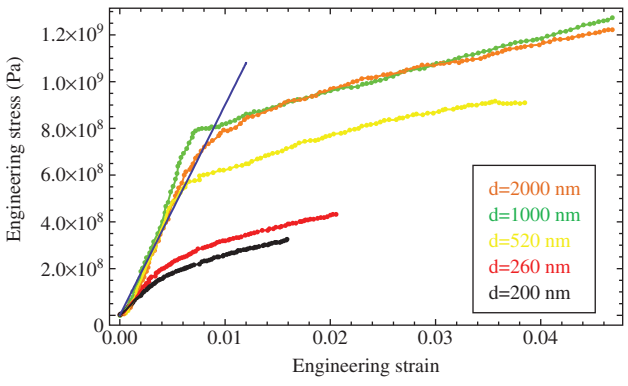

Figure 5: Recalculated engineering stress-strain graphs during $Pd_{77}Si_{23}$ metallic glass micropillar compression using Eq. (3). The slope of the straight line provides a modulus value of 90 GPa.

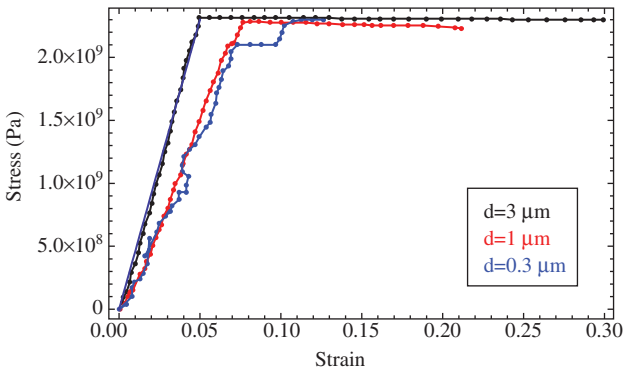

Figure 6: Engineering stress-strain graphs during Zr-based metallic glass micropillar compression [18]. The slope of the straight line provides a modulus value of 40–46 GPa.

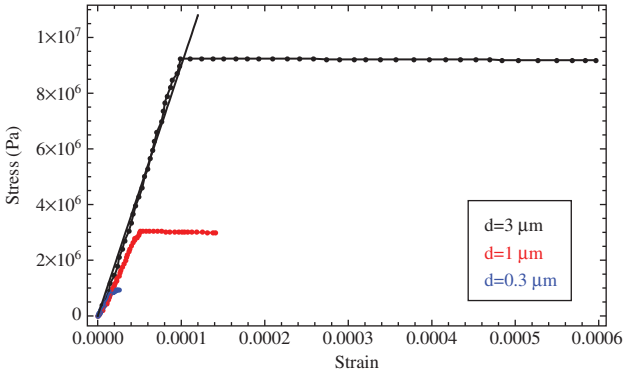

Figure 7: Recalculated engineering stress-strain graphs during Zr-based metallic glass micropillar compression using Eq. (3). The slope of the straight line provides a modulus value of 90 GPa.

the pillar and substrate are not two different materials in contact but, in fact, are one that is subject to deformation as a whole. As a result, the calculation of strain involves taking into account the total thickness of the pillar and substrate. The application of the above correction to experimental data eliminates two previously unexplained discrepancies. The first is the difference observed in the initial slopes of the stress-strain graphs. This fact should point to different elastic moduli for specimens of the same material but different sizes, which contradicts the elastic modulus being a material constant. Second, the measured elastic moduli were significantly lower than the bulk values. Future experiments should provide more inputs to better facilitate corrections to the calculation of strains.

Acknowledgments: Financial support from the Greek Secretariat of Research and Technology through the research programs ERC-13 (IL-GradMech-ASM) and ARISTEIA II (5152 – SEDEMP) is gratefully acknowledged.

References

[1] Tabor D. *The Hardness of Metals*. Oxford University Press: Oxford, UK, 2005.
[2] Uchic MD, Dimiduk DM, Wheeler R, Shade PA, Fraser HL. *Scr. Mat*. 2006, 54, 759–764.
[3] Greer JR, Nix WD. *Phys. Rev. B* 2006, 73, 245410 (1–6).
[4] Volkert CA, Lilleodden CT. *Philos. Mag*. 2006, 86, 5567–5579.
[5] Uchic MD, Dimiduk DM, Florando JN, Nix WD. *Science* 2004, 305, 986–989.
[6] Dimiduk DM, Uchic MD, Parthasarathy TA. *Acta Mater*. 2005, 53, 4065–4077.
[7] Kiener D, Motz C, Schöberl T, Jenko M, Dehm G. *Adv. Eng. Mater*. 2006, 8, 1119–1125.
[8] Nix WD, Greer JR, Feng G, Lilleodden ET. *Thin Solid Films* 2007, 515, 3152–3157.
[9] Maaß R, Petegem SV, Swygenhoven HV, Derlet PM, Volkert CA, Grolimund D. *Phys. Rev. Lett*.2007, 99, 145505–145511.
[10] Schuster BE, Wei Q, Zhang H, Ramesh KT. *Appl. Phys. Lett*. 2006, 88, 103113 (1–3).
[11] Volkert CA, Lilleodden ET, Kramer D, Weissmuller J. *Appl. Phys. Lett*. 2006, 89, 061920 (1–3).
[12] Biener J, Hodge AM, Hayes JR, Volkert CA, Zepeda-Ruiz LA, Hamza AV, Abraham FF. *Nano Lett*.2006, 6, 2379–2382.
[13] Konstantinidis AA, Aifantis KE, de Hosson JTM. *Mater. Sci. Engng. A* 2014, 597, 89–94.
[14] Greer JR, Oliver WC, Nix WD. *Acta Mater*. 2005, 53, 1821–1830.
[15] Fei H, Abraham A, Chawla N, Jiang H. *J. App. Mech*. 2012, 79, 061011–2.
[16] Tönnies D, Maaß R, Volkert CA. *Adv. Mater*. 2014, 26, 5715–5721.
[17] Schuster BE, Wei Q, Hufnagel TC, Ramesh KT. *Acta Mater*. 2008, 56, 5091–5100.
[18] Dubach A, Raghavan R, Löffler JF, Michler J, Ramamurty U. *Scripta Mater*. 2009, 60, 567–570.
[19] Kim PC, Suh JY, Wiest A, Lind ML, Conner RD, Johnson WL. *Scripta Mater*. 2009, 60, 80–83.